

Marine optical measurements of a mucilage event in the northern Adriatic Sea

Jean-François Berthon and Giuseppe Zibordi

Marine Environment Unit of the Space Applications Institute, Joint Research Centre of the E. C., TP272, 21020 Ispra, Italy

Stanford B. Hooker

NASA/Goddard Space Flight Center, Laboratory for Hydrospheric Processes, Greenbelt, Maryland 20771-5000

Abstract

Optical measurements performed during the summer of 1997 from an off-shore oceanographic tower in the northern Adriatic Sea in the presence of mucilage matter are presented. These measurements include apparent (diffuse attenuation coefficient, reflectance) and inherent (absorption and beam attenuation coefficients) optical properties of the water column at several wavelengths. The presence of mucilage layers (which was confirmed by divers) was associated with unique, very sharp subsurface maxima in the vertical distribution of both apparent and inherent optical properties. These layers were characterized by very high values of the diffuse attenuation coefficient of upwelling radiance and the beam attenuation coefficient, as well as the ratio of the scattering-to-absorption coefficients at all wavelengths. The mucilage data were compared to nonmucilage observations and two situations came out regarding surface reflectance ratios: (a) When the mucilage was in (vertically narrow) subsurface layers, mucilage events could not be distinguished from nonmucilage situations; and (b) When the mucilage was more homogeneously distributed throughout the water column and, in particular, approaching the surface, there was a detectable difference with respect to nonmucilage water. However, the data set is small, and the detection capability is based on a small difference, so the variance in nonmucilage water properties may still mask the properties of the mucilage-contaminated water.

During the summer of 1997, the northern Adriatic Sea was the site of a mucilage event. This outbreak was the first since the more intense 1988–1991 events. This recurrent phenomenon (Vollenweider et al. 1995) is represented by an intense production of organic gelatinous material which form suspended aggregates of varying sizes and shapes. The evolution of the phenomenon is thought to begin with small flocs in the order of millimeters, and end with strings and sheets of a few centimeters or even clouds on the order of meters. This development sequence is initiated by abnormal exudation of polysaccharide chains by phytoplankton, in particular, some specific diatoms. The chains are followed by the formation of colloids, and then, through successive aggregation, bigger particulate assemblages. The most striking stage is

their occasional presence at the surface as floating grayish to brownish strings and sheets.

The environmental conditions needed for the initial phytoplankton physiological manifestation, as well as for the aggregation processes, are not well understood, but the result is the aggregates become suspended micro-ecosystems with their own particular composition in protozoa, bacteria, phytoplanktonic algae, etc. The resulting biological activity, together with hydrodynamic forces and the proportions of living organisms to mucus, establish the vertical distribution of mucilage in the water column. Although some risks for human health may exist, linked in particular to the possible concentration of toxic allochthonous compounds within this matrix, a major negative effect of the phenomenon is the damage caused to the tourism industry from floating mucilage concentrated near the coast. Of particular interest to coastal communities is forecasting the development and motion of mucilage production events.

Remote sensing (satellite or airborne) techniques may provide a useful tool for monitoring and surveying the extent and intensity of mucilage events, given knowledge of the spectral properties of the different stages of development. Use of remotely sensed information in the visible and the infrared has already been proposed (Zambianchi et al. 1992; Tassan 1993) for detecting floating mucilage. In this case, the bright floating patches contribute to enhancement of the surface reflectance signal at all wavelengths. Nevertheless, this stage is only one phase in mucilage development, and it may be of interest to investigate the possibilities of detecting and monitoring subsurface stages.

To this end, we present a unique bio-optical data set collected during recurring measurement campaigns performed from the Acqua Alta Oceanographic Tower in the northern

Acknowledgments

CoASTS is a cooperative project between the Joint Research Centre and the Italian National Research Council. The authors are very grateful to Stefania Grossi, Dirk van der Linde, and Cristina Targa from JRC for performing laboratory analyses or in situ sampling. Pier Luigi Cova, Claudia Ramasco, Barbara Sapino, and Alessandro Vianello from the CNR-ISDGM, led by Luigi Alberotanza, are duly acknowledged for their competent and essential contributions in the field campaigns. A special acknowledgment is also owed to the tower crew, Armando Penzo, Narciso Zennaro, Daniele Penzo, and Gianni Zennaro for their logistical support during each field campaign. The authors are also very grateful to Stelvio Tassan for helpful comments as well as to the two anonymous reviewers for their constructive criticisms and suggestions, and to the Associate Editor, Dr. Richard Geider, whose review helped a lot in making the manuscript more concise.

This work has been partially supported by the European Commission through the Coastal Monitoring and Management Project (SAI-X05) and by NASA through grant NCC5-371.

Adriatic Sea during a mucilage event in the summer of 1997. The objective of the data analysis is to determine what aspects, if any, of the mucilage event can be uniquely identified using optical instruments. The implications of these results for the use of ocean color remote sensing in the monitoring of mucilage, in particular when present at depth, are discussed.

Data and methods

The CoASTS time series—Within the field campaigns of the Coastal Atmosphere and Sea Time-Series (CoASTS) Project, which started in October 1995 and continues to-date, atmospheric and marine measurements are periodically performed at the Acqua Alta oceanographic tower. The tower is operated by the Italian National Research Council and is located in the northern Adriatic Sea approximately 15 km southeast of the city of Venice (12.51°E, 45.31°N) in approximately 17 m of water (Zibordi et al. 1995). Measurement campaigns last a few days and take place every 2–4 weeks, depending on the season, and can include from 3–10 sets of measurements or stations. The measurements include in-water optical profiles, water samples at different depths (0, 8, and 14 m) for biogeochemical analyses, temperature and conductivity profiles, sky radiance and sun irradiance, and meteorological data. For the present work the following measurements from selected campaigns are used:

1. Underwater upwelling radiance $L_u(\lambda, z)$ at nadir and irradiance $E_u(\lambda, z)$, plus downwelling irradiance $E_d(\lambda, z)$ (all at 412, 443, 490, 510, 555, 665, and 683 nm), taken with OCR-200 and OCI-200 Satlantic radiometers. From these measurements, we derived the spectral diffuse attenuation coefficients for upwelling radiance and downwelling irradiance, $K_{Lu}(\lambda, z)$ and $K_{Ed}(\lambda, z)$, respectively, as well as the reflectance, $R(\lambda, z) = E_u(\lambda, z)/E_d(\lambda, z)$ with a vertical resolution of 1 m.

2. In situ beam attenuation $c(\lambda, z)$ and absorption $a(\lambda, z)$ coefficients (all at 412, 440, 488, 510, 555, 630, 650, 676, and 715 nm) taken with a Wetlabs AC-9. The values presented in this study do not include the contribution from pure seawater and correspond to mean values within 1-m thick layers. Scattering correction to the measured absorption was performed following the method of Zaneveld et al. (1992).

3. Water temperature and conductivity taken with an Idronaut CTD.

4. Pigment concentrations measured with the high performance liquid chromatography (HPLC) method (JGOFS 1994). Only the concentration of Chl *a* (including chlorophyllide *a*), denoted as [Chl] and expressed in mg m^{-3} , is used hereafter.

5. Total suspended matter concentration, denoted as [TSM] and expressed in g m^{-3} , measured by the dry weight method (Strickland and Parson 1972).

6. In vivo pigmented and nonpigmented particulate matter absorption spectra, $a_{ph}(\lambda)$ and $a_{dp}(\lambda)$, using the Tassan and Ferrari (1995) method.

7. Colored dissolved organic matter absorption spectra, $a_{ys}(\lambda)$ as in Ferrari et al. (1996).

The first three are derived from continuous profiles,

Table 1. Chlorophyll *a* [Chl], total suspended matter [TSM], colored dissolved organic matter absorption coefficient at 400 nm ($a_{ys}[400]$) and ratio of the in situ scattering and absorption coefficients at 440 nm ($b/a[440]$) at 0, 8, and 14 m for the selected stations. Optical profile M1 was performed one hour after the water sampling. Note that the different quantities are corresponding to the depths of water sampling and thus are not systematically representative of high attenuation layers described in the text.

CoASTS station	Present numeration	Sampling depth (m)	[Chl] (mg m^{-3})	[TSM] (g m^{-3})	a_{ys} (400) (m^{-1})	b/a (440)
30s4.04 9 Jul 1997	M1	0.0	0.982	0.67	0.152	8.4
		8.0	0.887	0.87	0.119	20.2
		14.0	1.340	0.53	0.164	4.4
31s5.01 30 Jul 1997	M2	0.0	2.842	2.58	0.163	7.5
		8.0	1.314	1.42	0.115	6.8
		14.0	1.152	2.42	0.204	4.8

whereas, the last four are from discrete water samples collected at certain depths.

Selection of the mucilage data—The abundance of mucilage peaked during the months of July and August 1997 at the tower site. Divers reported underwater visual observations of mucilage, mucus aggregates were found on the submersible instruments, and, on some occasions, ribbons of floating mucilage disks (diameter of the order of tens of cm) were seen after boats passed by. These observations—simultaneously made in other areas of the northern Adriatic Sea—were qualitatively very similar to those reported during previous events in the Adriatic and Tyrrhenian Seas (Innamorati 1995; Rinaldi et al. 1995). During these months, and particularly in early July, the vertical distribution of optical properties showed unusual patterns with strong peaks at depths never seen during the preceding campaigns.

The stations showing the most noticeable effect of mucilage on underwater optical properties were extracted from the 1997 CoASTS archive to form a mucilage data set. The mucilage data set includes profiles from campaigns 30 (08–10 July), 31 (29–31 July), and 32 (20 August). In particular, two stations, renamed M1 and M2 (see Table 1) will be presented in detail.

Results and discussion

Vertical distribution of the optical properties in the water column—Figure 1 presents two vertical profiles of $K_{Lu}(\lambda, z)$ at 443, 555, and 665 nm together with $c(\lambda, z)$ and $a(\lambda, z)$ (at 440, 555, and 676 nm) typical of the mucilage campaigns (stations M1 and M2). The use of $K_{Lu}(\lambda, z)$ has been chosen rather than $K_{Ed}(\lambda, z)$, because upward radiance is more sensitive than downward irradiance to changes in the vertical distribution of bio-optical properties in the water column, since it is less influenced by the direct light component.

On these profiles, subsurface mucilage is evident as strong maxima of K_{Lu} and c at depths around 8–9 m. At these maxima, $K_{Lu}(443)$ varies between 0.45–1.40 m^{-1} and $K_{Lu}(555)$

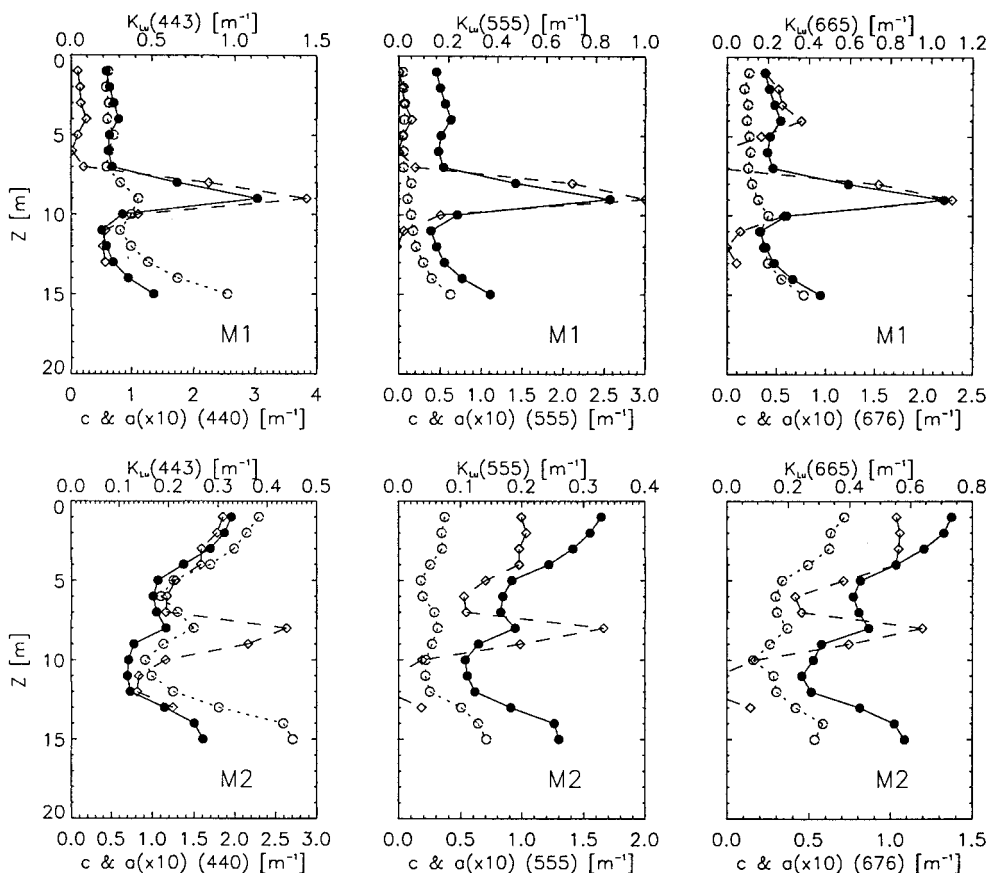


Fig. 1. Vertical profiles of the diffuse attenuation coefficient for upwelling radiance $K_{Lu}(\lambda, z)$ (dashed line and open diamonds) and of the in situ beam attenuation $c(\lambda, z)$ (solid line and solid circles) and absorption $a(\lambda, z)$ (dotted line and open circles) coefficients at 443 (440 for c and a), 555 and 665 (676 for c and a) nm. See text and Table 1 for the explanation of station numbers.

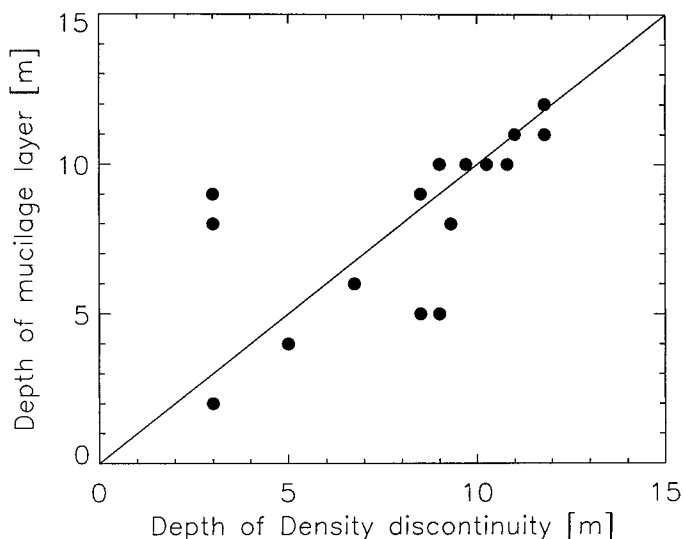


Fig. 2. Vertical position of the subsurface mucilage layer versus depth of the main density discontinuity.

between 0.30–1.00 m^{-1} (M2 and M1); $c(440)$ between 1.20–3.00 m^{-1} , whereas $a(440)$ ranges between 0.11–0.15 m^{-1} . The width of these maxima is relatively constant and equal to approximately 3 m. In rare cases (e.g., M2), mucilage was observed floating on the surface, and this usually coincided with the passage of boats, but this material usually sank within several minutes. Alldredge and Crocker (1995) observed that mucous aggregates could occur at density gradients increasing by only one to three units of density. Figure 2 presents, for all the stations belonging to the mucilage data set, the plot of the position of these observed subsurface maxima of K_{Lu} and c versus the depth where the density was one unit higher than the mean density within the surface layer. A good correspondence can be observed between the two depths, consistent with Alldredge and Crocker's (1995) observation (see also the following Fig. 3).

Good coupling between $K_{Lu}(\lambda, z)$ and $c(\lambda, z)$, and to a lesser extent $a(\lambda, z)$, is evident at all wavelengths (Fig. 1). For station M1, $a(\lambda, z)$ is much less correlated with $K_{Lu}(\lambda, z)$ in the red part of the spectrum than in the blue and green, except near the bottom, suggesting that the amount of pigmented material embedded in these highly attenuating (mucilage) layers was less than for the other stations ([Chl] was also lower for station M1 than for M2 as shown in Table 1).

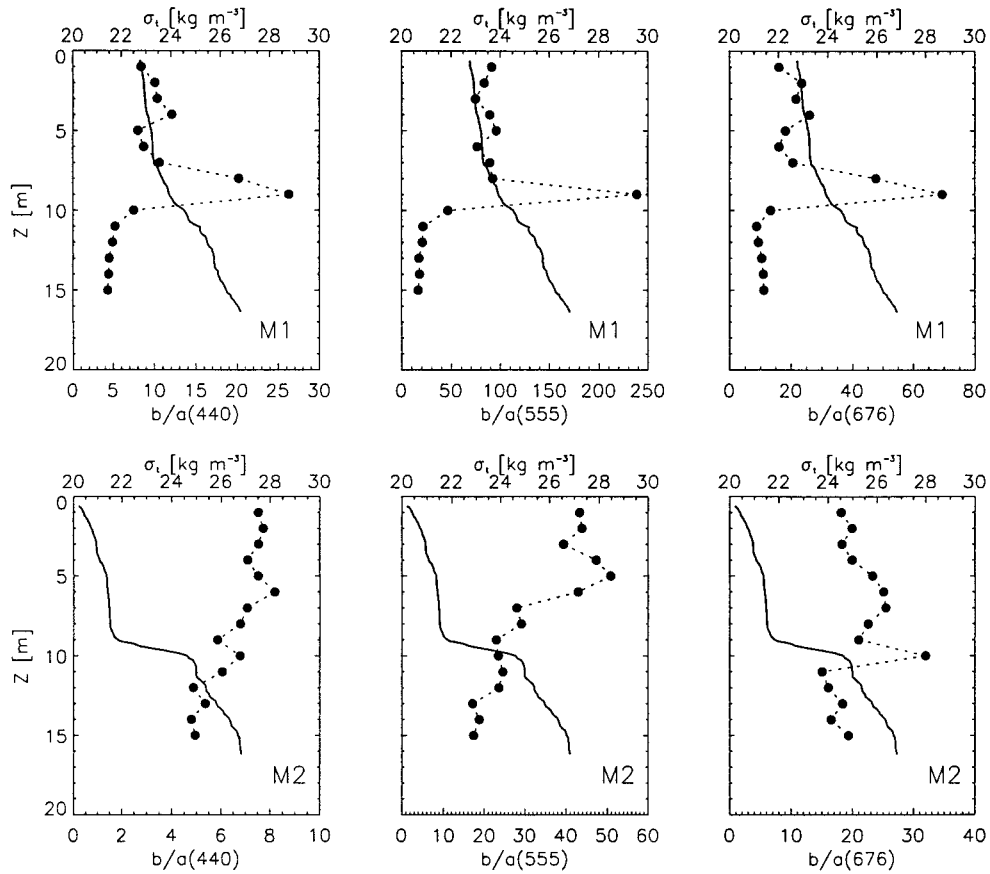


Fig. 3. Vertical profiles of the ratio $b(\lambda, z)/a(\lambda, z)$ (where $b = c - a$) (dotted line and solid circles) for the same wavelengths as in Fig. 1 and vertical profiles of density (solid line).

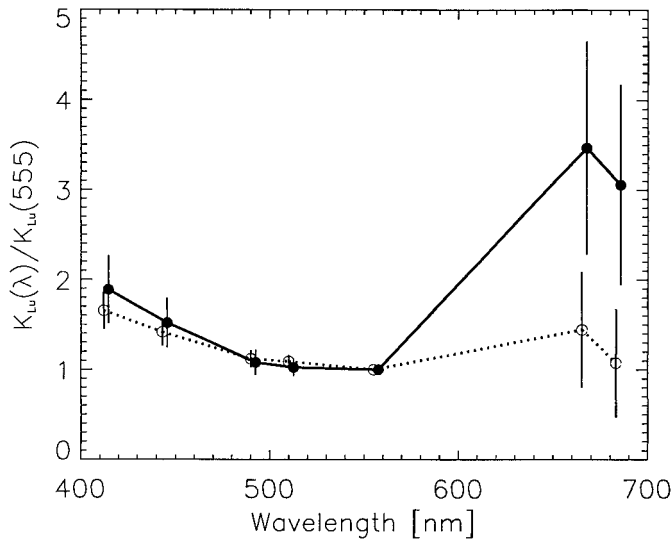


Fig. 4. Average spectra of the diffuse attenuation coefficient for upwelling radiance, K_{Lu} , normalized to the value at 555 nm, computed for 1-m thick layers. Dotted line and empty circles: mucilage data set; solid lines and solid circles: CoASTS 1995–1997 data set excluding the mucilage campaigns 30, 31, and 32. Vertical bars around circles: ± 1 SD.

Obviously, $c(\lambda, z)$ and $a(\lambda, z)$ do not include the contribution of pure water itself (particularly elevated in the red), whereas $K_{Lu}(\lambda, z)$ does, but this contribution is depth independent. The good correspondence between passive (OCR-200) and active (AC-9) optical signals also shows the coherency of the derived vertical structure of $c(\lambda, z)$ and $a(\lambda, z)$; although, the mucilage matter probably perturbed the water flux inside the AC-9 chambers by aggregating on the external filters and increased the noise in the resulting recorded data.

Figure 3 presents the vertical distribution of the ratio $b(\lambda, z)/a(\lambda, z)$ (where $b = c - a$) for the same wavelengths as in Fig. 1. The b/a ratios are shown with density profiles, and it can be seen that very high values of b/a are indicative of the highly attenuating layers described earlier. At the depths of these layers, $b(440)/a(440)$ varies between 7 (M2) and 27 (M1), whereas, $b(555)/a(555)$ varies from 30 to 250 (for the same stations). As a matter of comparison, two situations of high [TSM] concentration at the surface (thus, susceptible to exhibit high-scattering values) recorded during the CoASTS program (4.13 and 2.27 g m^{-3} in April 1997 and February 1998, respectively) presented b/a ratio maximum values of 19 and 8 at 440 nm and 85 and 33 at 555 nm. The major difference between mucilage and nonmucilage layers, therefore, is seen here most clearly in the green part of the spectrum.

Spectral characteristics of K_{Lu} measured in the mucilage layers—Figure 4 shows the average normalized (to 555

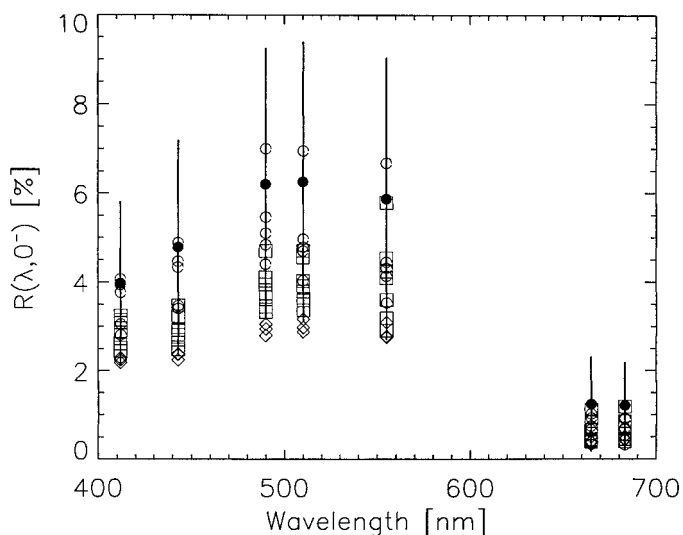


Fig. 5. Spectra of the irradiance reflectance immediately below the surface, $R(\lambda, 0^-)$. Open symbols: circles (campaign 30), squares (campaign 31), diamonds (campaign 32). Solid circles and bars: mean ± 1 SD computed for the leftover CoASTS stations (i.e., campaigns of the first two years excluding campaigns 30, 31, and 32).

nm) $K_{Lu}(\lambda)$ spectra computed for the mucilage data set from the individual spectra measured at the depth of the main subsurface maximum (dashed line and empty circles with bars indicating ± 1 SD). For comparison purposes the average spectrum computed for the CoASTS data set (1995–1997) excluding the mucilage campaigns is also shown (solid line and circles). For this last, individual $K_{Lu}(\lambda)$ were computed within an optically homogenous surface layer, the maximum values of [TSM], and [Chl] being generally observed within this surface layer. The CoASTS spectrum is presented shifted by 2.5 nm in order to better visualize the differences.

Both average spectra appear very similar in the range 490–555 nm with a relatively flat shape and a very slight minimum at 555 nm. Between 490 and 412 nm values are then increasing with a slightly lower slope for the mucilage spectrum than for the CoASTS one, resulting in a $K_{Lu}(412)/K_{Lu}(555)$ ratio of about 1.65 at 412 nm (versus 1.9 for CoASTS). Both situations are completely differentiated in the red part of the spectrum around the $K_{Lu}(665)/K_{Lu}(555)$ ratio of 2. Globally, the average mucilage spectrum results flatter than the CoASTS one in the range 412–665 nm.

Surface reflectances—Figure 5 shows the reflectance spectra, $R(\lambda, z) = E_u(\lambda, z)/E_d(\lambda, z)$, immediately below the surface, $R(\lambda, 0^-)$, for all stations pertaining to the mucilage campaigns 30, 31, and 32 (indicated by the open symbols). Also shown is the average spectrum (solid circles with bars indicating ± 1 SD) computed for the CoASTS data set excluding the mucilage campaigns. Apart from one station in campaign 30, the mucilage reflectance values are systematically lower than the mean CoASTS spectrum; although, the mucilage data are within ± 1 SD of the mean spectrum.

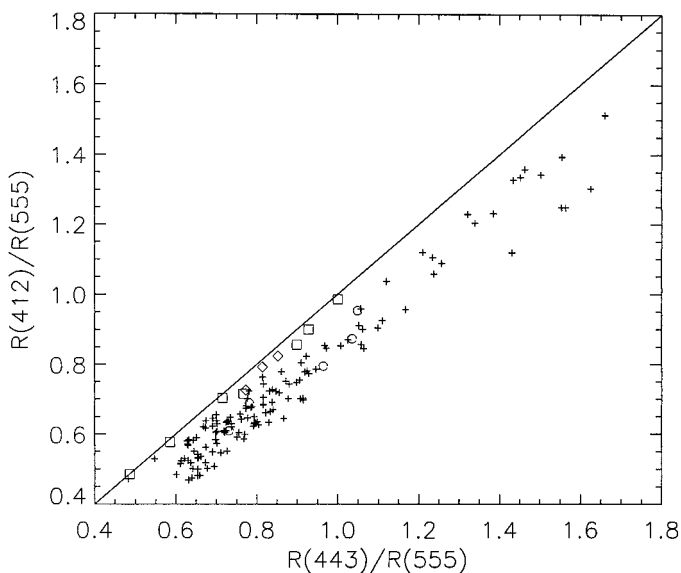


Fig. 6. Plot of the ratio of the reflectances $R(\lambda, 0^-)$ at 412 and 555 nm versus the ratio of the reflectances $R(\lambda, 0^-)$ at 443 and 555 nm. Open symbols: circles (campaign 30), squares (campaign 31), diamonds (campaign 32). Plus symbols: other CoASTS stations. The solid line represents the 1:1 ratio.

Apart from campaign 32 (open diamonds) for which reflectances at 490 and 510 nm are slightly lower than the mean -1 SD, no specific characteristics indicating the presence of mucilage could be detected from the absolute surface signal. Moreover, instead of presenting an increase of the surface signal, as observed from satellite data for floating mucilage (Tassan 1993), the measured surface signal is globally lower with respect to the mean. The high attenuation due to the presence of both mucilage and high surface values of [TSM] or [Chl] (in particular during July 1997) may explain these relatively low reflectances.

Figure 6 shows the $R(412)/R(555)$ ratio versus the $R(443)/R(555)$ ratio for the mucilage stations (open symbols) as well as for all the other CoASTS stations (plus symbols). It can be seen that for a given $R(443)/R(555)$ ratio, the $R(412)/R(555)$ ratio is slightly higher for the mucilage stations of campaigns 31 and 32 (open squares and diamonds) whereas stations from campaign 30 (open circles) do not show any distinct behavior. The latter are the ones for which the highly attenuating mucilage layers were observed at depths of a few meters, without any apparent influence on the surface signal. The ratios presented here ensured the best distinction between the two groups of stations. It has to be emphasized that such a distinction is based on in situ reflectance measurements performed at a sampling point. Since we lack information on their spatial distribution we cannot assess whether these underwater “ribbons” or “agglomerates” would have an optical contribution within satellite pixels of about 1×1 km (e.g., SeaWiFS resolution at nadir). However, mucilage structures (ribbons of 100–200-m width and a few km length or agglomerates of 30–100 km²) when floating at surface could be very well identified using Landsat-Thematic Mapper imagery (30×30 m pixels) (Zambianchi et al. 1992; Tassan 1993). They still had a significant con-

tribution to the total signal within 1×1 km pixels of AVHRR imagery (Zambianchi et al. 1992) or within boxes of 33×33 pixels (i.e., 1.1×1.1 km) of Landsat-Thematic Mapper (Tassan 1993).

When considering the surface signal (absolute reflectance or reflectance ratios immediately below the surface), mucilage in (vertically narrow) subsurface layers, could not be distinguished from nonmucilage waters. When mucilage events could be discriminated from nonmucilage situations, the mucilage was also present near the surface. Although the difference between mucilage and nonmucilage waters was small, the use of both $R(412)/R(555)$, and $R(443)/(555)$ ratios was found to give the best segregation index. However, the data set analyzed is small, and the detection capability is based on a small difference, so the variance in nonmucilage water properties may still mask the properties of the mucilage-contaminated water. Also, it can be that no real unique optical characteristics has been found for mucilage because they are complex (and not well known yet) assemblages with varying proportions of living and nonliving material. In addition, the results indicate the identification of mucilage using remote sensing in the visible part of the spectrum may be particularly difficult at stages other than the bright surface or near-surface floating sheets.

References

- ALLDREDGE, A. L., AND K. M. CROCKER. 1995. Why do sinking mucilage aggregates accumulate in the water column? *Sci. Total Environ.* **165**: 15–22.
- FERRARI, G. M., M. D. DOWELL, S. GROSSI, AND C. TARGA. 1996. Relationship between the optical properties of chromophoric dissolved organic matter and total concentration of dissolved organic carbon in the southern Baltic Sea region. *Mar. Chem.* **55**: 299–316.
- INNAMORATI, M. 1995. Hyperproduction of mucilages by micro and macro algae in the Tyrrhenian Sea. *Sci. Total Environ.* **165**: 66–81.
- JGOFS. 1994. Protocols for the Joint Global Ocean Flux Study Core Measurements. Intergovernmental Oceanographic Commission, Scientific Committee on Oceanic Research. Manual and Guides, UNESCO **29**: 91–96.
- RINALDI, A., R. A. VOLLENWEIDER, G. MONTANARI, C. R. FERRARI, AND A. GHETTI. 1995. Mucilages in Italian seas: The Adriatic and Tyrrhenian Seas, 1988–1991. *Sci. Total Environ.* **165**: 165–183.
- STRICKLAND, J. D. H., AND T. R. PARSONS. 1972. A practical handbook of sea water analysis, 2nd ed. Fisheries Research Board of Canada **167**: 181–184.
- TASSAN, S. 1993. An algorithm for the detection of the white-tide (“Mucilage”) phenomenon in the Adriatic Sea using AVHRR data. *Remote Sens. Environ.* **45**: 29–42.
- , AND G. M. FERRARI. 1995. An alternative approach to absorption measurements of aquatic particles retained on filters. *Limnol. Oceanogr.* **40**: 1358–1368.
- VOLLENWEIDER, R. A., G. MONTANARI, AND A. RINALDI. 1995. Statistical inferences about the mucilage events in the Adriatic Sea, with special reference to recurrence patterns and claimed relationship to sun activity cycles. *Sci. Total Environ.* **165**: 213–224.
- ZAMBIANCHI, E., C. CALVITTI, P. CECAMORE, F. D’AMICO, E. FERULANO, AND P. LANCIANO. 1992. The mucilage phenomenon in the northern Adriatic Sea, summer 1989: A study carried out with remote sensing techniques, p. 581–598. *In* R. A. Vollenweider, R. Marchetti, R. Viviani [eds.], Marine coastal eutrophication. Proceedings of an International Conference. Bologna, Italy, 21–24 March 1990. *Sci. Total Environ. Suppl.*
- ZANEVELD, J. R. V., J. C. KITCHEN, A. BRICAUD, AND C. MOORE. 1992. Analysis of *in situ* spectral absorption meter data. *Ocean Optics XI, Proc. Soc. Photo-Optical Instrum. Eng. (SPIE)* **1750**: 187–200.
- ZIBORDI, G., V. BARALE, G. M. FERRARI, N. HOEPPFNER, D. W. VAN DER LINDE, L. ALBEROTANZA, P. L. COVA, AND C. RAMASCO. 1995. Coastal Atmosphere and Sea Time-Series Project (CoASTS). An Ocean Colour Remote Sensing Calibration/Validation Project. 3rd Thematic Conference on Remote Sensing for Marine and Coastal Environment. ERIM, 18–22 September 1995, Seattle.

Received: 16 February 1999
Amended: 24 September 1999
Accepted: 1 October 1999